Classification of black plastic using active thermography

Kevin Schmitz[1*], Nina Shpakova[1], Andreas Keller[1], Udo Netzelmann[1]

1 Fraunhofer Institute for Nondestructive Testing IZFP, Saarbrücken, Germany

* Corresponding Author: Campus E3.1, 66123 Saarbrücken, E-Mail: kevin.schmitz@izfp.fraunhofer.de

Keywords: machine learning, recycling, sorting black plastic, thermography, waste management

Abstract

Sustainability is undoubtedly one of the most important goals in modern society and has a major impact on economic and political decisions. One of the strategies towards sustainability is the European Green Deal. A key policy initiative that determines the regulatory landscape supporting the European Green Deal is the Circular Economy Action Plan (CEAP) (EC, 2020), whose objective is to reduce the EU's consumption footprint and double its circular material use rate in the coming decade, while boosting economic growth. Specific actions were launched in several areas, including electronics and ICT[1], packaging, plastics and textiles. An important segment of a circular economy, especially in waste management, is the sorting and recycling of materials. To raise levels of high-quality recycling, improvements are needed in waste collection and sorting.

The sensor systems currently available on the market for sorting plastics in waste management largely rely on near-infrared (NIR) and short-wave infrared (SWIR). However, the sorting of black plastics, including those manufactured in the automotive field, remains problematic with these systems. The task of sorting these black plastics from the shredder light fraction poses a demanding challenge to sorters.

1 Information and communications technology

As part of the Fraunhofer lighthouse project »Waste 4 Future« (W4F), which deals with the holistic improvement of plastic recycling, an active thermography system for distinguishing different plastic materials was developed. In this context, three black materials from the shredder light fraction were investigated on a running conveyor belt. The sample set consisted of ten defined samples each of the material polypropylene glass fiber (PP-GF) as well as two polyamide glass fiber materials, namely PA6-GF and PA66-GF. The samples were heated up by using an infrared heater. An infrared camera mounted at a fixed distance above the conveyor belt was able to record the cooling curve of the samples over time. Due to their different heat conduction properties, different materials should have different heating, as well as cooling characteristics. By analyzing the cooling curves, it was possible to identify characteristic patterns in different materials. Feature extraction enabled the quantification of the observations, which were then processed by machine learning algorithms. Using three samples per material as validation data, a pixel-wise f1-score above 97% was achieved. When using majority decision per sample, every sample could be classified without any misclassifications.

The knowledge gained from active thermography opens up promising perspectives for integration with the current state-of-the-art sensor technologies. Thermography systems can contribute to the further development of sorting systems and play a crucial role in improving the recycling process, especially with regard to black plastics. This approach can contribute to enabling more precise sorting and thereby more efficient recycling of plastics.

1 Introduction

Global warming and the increasing depletion of resources are major challenges society is facing today and in the future. In this context, the pursuit of sustainability has become an undeniable priority and acts as a central goal for responsible development. Both political and economic decisions are significantly influenced by the efforts to achieve these goals. To accelerate the transformation of the European Union towards climate neutrality and resource efficiency, the “European Green Deal” was launched at the beginning of 2020. One important initiative of this sustainability strategy is the Circular Economy Action Plan (CEAP) (EC, 2020). The CEAP focuses on reducing the environmental footprint within the EU and proposes various measures in different areas. A central aspect of this plan is the sustainable circular economy, which aims to minimize the consumption of resources and extend the life cycle of products. The recycling of materials in particular plays a key role in this, which means that the recycling process is not only seen as a waste management strategy, but also as an essential part of realizing the goals of the CEAP. In this context, CEAP aims to double the use of recycled materials over the next ten years. This ambitious measure is intended to intensify the use of recycled raw materials in production and thus make a significant contribution to conserving resources and reducing emissions. Doubling the use of recycled material emphasizes the ongoing shift towards a sustainable economy and highlights the need to strengthen the recycling process as a central element in the circular economy.

Sorting is undoubtedly a crucial segment of an effective recycling process. The precise and clean separation of recyclable materials plays a key role in the process of increasing their usage. Accurate sorting not only enables more efficient reuse of materials, but also contributes significantly to improving the quality of recycled products. By ensuring separation by type, impurities can be minimized, which ultimately leads to higher quality and more versatile recycled materials. This focus on precision in sorting is therefore key to making the circular economy effective and sustainable.

The sorting of plastics has seen significant technological advances in recent years (Gundupalli et al., 2017). The focus here is on near-infrared (NIR) and short-wave infrared (SWIR) based techniques (Chen et al., 2020; Sensors Unlimited). These technologies enable fast and precise identification of plastic types by analyzing the absorption in the respective wavelengths. However, the sorting of black plastics remains particularly challenging, as they are more difficult to recognize in the near-infrared range (Masoumi et al., 2012; Rozenstein et al., 2017). Fundamental research regarding the usage of terahertz waves to separate multiple black plastics is currently being conducted and could prove beneficial in the future (Brandt et al., 2016). Lastly, tracer-based sorting (TBS) is already employed by some plastics manufacturers (Polysecure GmbH), wherein plastic additives or fluorescent markers are added to a compound, resulting in a separation by type and area of application of the plastic (e.g. food packaging) (Olscher et al., 2022). Despite all the progress, challenges remain, particularly due to different additives (Jehanno et al., 2022), multilayer packaging (Schmidt et al., 2022) and the ever-increasing amount of plastics that are being used (Stegmann et al., 2022). The development of technologies that address these challenges is crucial to increasing recycling efficiency and ensuring the sustainable utilization of plastic waste.

There exists a wide variety of analytical methods to characterize and classify polymers, e.g. thermogravimetric analysis (TGA) or differential scanning calorimetry (DSC) (Menczel & Prime, 2009). However, the use of infrared thermography to classify polymers is an underdeveloped field of research, but with possibly promising results (Aujeszky et al., 2017).

In the Fraunhofer lighthouse project »Waste 4 Future« (W4F) seven Fraunhofer institutes are working together to achieve a holistic improvement in the recycling process. The efficient utilization of carbon contained in plastics should result in high-quality output materials. Using an evaluation model and innovative sorting technology, the project aims to efficiently recycle plastics in a circular economy and reduce thermal utilization. Economic aspects and regulatory requirements are also taken into account in order to develop a sustainable business model. One part of the innovative sorting technology is a new approach using active thermography, which is explained in more detail below and the insights gained are described.

2 Active thermography

Other than in NIR spectroscopy around room temperature, infrared thermography in the thermal infrared range (about 2 to 15 µm wavelength) relies on the thermal emission of infrared radiation according to Planck's law. Besides the temperature of the object, its emissivity is a decisive factor. The reflectivity plays a minor role, in contrast to NIR spectroscopy. Polymers appearing black in the visible absorb visible and NIR light very well and convert the light energy efficiently into heat and then into thermal radiation. Active thermography uses short-time intentional heating of the sample beyond its initial temperature, e. g. by a strong optical light source. Sample surface heating increases the infrared emission and leads to a heat flow from the surface into the depth of the object. The resulting increase in transient surface temperature is influenced by its thermal conductivity, its density, and its specific heat capacity. In addition, most polymers are usually semi-transparent in the thermal infrared. Their thermal radiation comes both from the surface and from the volume. A short time after optical heating, the radiation from the surface-near region is dominant and more dependent on the spectral properties in the thermal infrared than at later times (Jones Roger W. & McClelland John F., 1989), it is therefore useful to record the time dependence of the infrared radiation.

By combining the effects of thermal diffusion, optical absorption, and emission of thermal radiation, a differentiation between different polymer materials should be possible. In order to accurately capture the effects described, the infrared sensor FLIR A35 was chosen. The operational characteristics of this camera, including the spectral range, were deemed sufficient to effectively fulfil the requirements. An overview of the technical specifications of the FLIR A35 camera can be found in Table 1.

Tab. 1: Thermal camera specifications

Camera type	Focal Plane Array, uncooled VOX-microbolometer
Framerate	60 fps
Resolution	320 x 256 px
Spectral	7.5-13 µm
Distance camera-sample	62 cm
Thermal sensitivity NEDT	50 mK
Field of View	48 ° x 39 °

3 Design of Experiment

The implementation of a proper design of the experiment is crucial in researching new measurement techniques. A proper and well-thought experimental design ensures that the objective of the experiment is achieved with high accuracy and efficiency. Measuring quantities is always an integral collection of data across many factors. Therefore, it is important to systematically control the variables, minimize the biases, and enhance the statistical validity of the measurement. A disciplined approach increases the reproducibility of results and ensures an identification of causal relationships, instead of correlations.

To ensure a stable measurement setup, the configuration was carefully planned and mechanically secured, preventing any alterations in distances throughout the project. A conveyor belt is moving the samples at a constant speed. This is a critical aspect, enabling the construction of a cooling curve for each pixel from a sequence of frames. The samples are transported to an infrared heater, actively introducing heat. Subsequently, the samples are transported further and enter the recording range of the infrared camera. By maintaining a fixed position and belt speed, uniform cooling times for the samples across all measurements are ensured. This standardized approach enhances the reliability and precision of the experimental outcomes. A schematic of the measurement setup is shown in the figure Fig. 1.

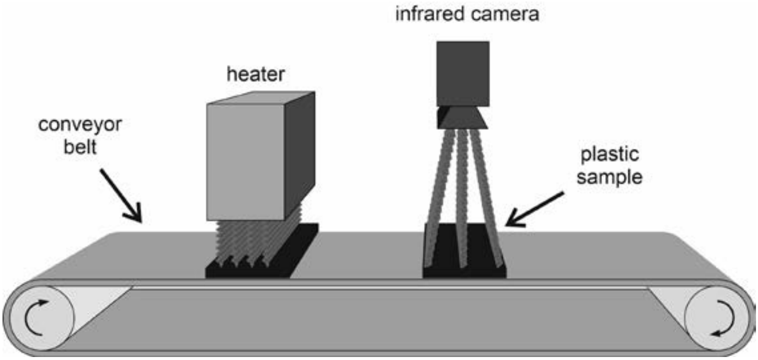

Fig. 1: Measurement setup schematic

With the setup being defined, it is essential to identify the most dominant influences that affect the whole measurement procedure. Once the influences relevant to this measurement have been identified, they must be classified. A list of influences including their categorization is shown in Fig. 2. Influencing factors are displayed in three different categories. The “star” marks the relevant information that is categorized as a measurement effect, which is the aim of the measurement. The wrench symbolizes influences that are marked as parameters, which means that they can be actively controlled by the measurement setup. The “warning sign” influences are non-predictable, not measurable or changing influences, and in real world applications especially not controllable, which can affect the measurement. In real-world applications, factors such as the sample geometry, ambient temperatures, and containments play significant roles but cannot be controlled by the sorting facilities. When analyzing the data, it can always happen that unknown influences exist, that may exhibit correlation over time. Factors like the self-heating of sensors or alterations in boundary conditions can influence the data over time. Additionally, the inherent inaccuracies in sensors contribute to what is commonly known as sensor scattering.

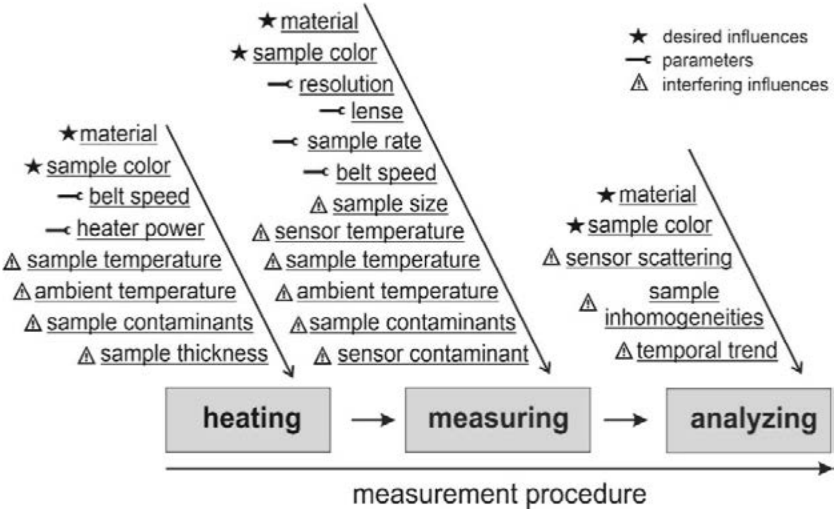

Fig. 2: Categorized major influences that affect the measurement

In the initial phase, it is crucial to optimize the parameters and set them to their best possible values, so that subsequent adjustments are no longer necessary. This initial optimization step effectively mitigates some of the influences. All interfering influences are kept constant, to attempt to maintain consistency along all the measurements. The first series of measurements therefore is made on clean samples with fixed dimensions, as well as controlled sensor-, sample- and ambient temperature.

The selection of samples must be chosen wisely to ensure a comprehensive representation of the desired influences (illustrated as “star” factors). This is essential to account for inhomogeneities and sensor scattering. These factors are difficult to control by other means and must therefore be included in the training process. The three polymers examined in this work are black due to the addition of carbon black to the batch and filled with 30 % glass fiber. The samples consist of a polyamide 66 (PA66-GF) (TECHNYL A216 V30 BLACK 21N by DOMO Chemicals, Leuna, Germany), a polyamide 6 (PA6-GF) (DOMAMID 6G30 BK, also by DOMO Chemicals) and a polypropylene (PP-GF) (Scolefin 53 G13-9 by Ravago Group, Arendonk, Belgium). All polymers were injection molded in the facility of Fraunhofer Institute for Structural Durability and System Reliability LBF. The geometrical shape is composed of a square with a side length 80 mm and a thickness of 3 mm and a triangle with the longest side of 90 mm. The triangular part is only used for numbering and touching the samples, whilst the square part is the actual analyzed area. This prevents measurement errors introduced by heat transfer through contact with the hand or by measuring the numbering of a sample instead of their cooling curve. An example of a sample can be seen in Fig. 3

Fig. 3: PA6-GF sample no.874

To ensure a minimum in variance between the samples, the injection molding process was kept running for a while before ten samples of a given material were produced in series. The thermal conductivity λ of the three analyzed polymers are shown in Table 2, taken from the matweb website (matweb).

Tab. 2: Thermal conductivity of the three analyzed polymers

Material	Thermal conductivity λ[W/mK]
PA66-GF	0.24-0.25
PA6-GF	0.25
PP-GF	0.27-0.331

Finally, in order to suppress the possible influence of temporal dependencies, a randomized sample sequence is selected. This approach eliminates dependencies in the data and contributes to a more robust and unbiased analysis.

4 Data analysis

Data analysis plays a central role in the measurement process, as it establishes a correlation between the measured data and the material properties. An essential process is preprocessing, which aims to amplify the desired effect while minimizing interfering influences. After pre-processing, the actual analysis is carried out using various machine learning (ML) techniques to identify patterns and correlate the data to its respective material.

4.1 Feature extraction

The conveyor belt is moving the samples at a consistent speed, and the camera takes frames with a constant frame rate that enables a precise calculation of the pixel shift, i.e. the distance traversed by the samples between the consecutive camera frames. As parts of the sample move out of the camera view, cooling curves are constructed for each pixel along the sample line by line, using a corresponding stack of the previously taken camera frames. The number of camera frames taken for each piece of the sample, i.e. the cooling curve resolution, depends on the conveyor belt speed and the camera frame rate. Greater resolution improves result precision, yet, finding a tradeoff is necessary for maximizing both the performance and the quality of the result. Since in most cases, the pixel shift is a non-integer number, linear interpolation was utilized while creating the cooling curves to enhance the accuracy of the results.

A polynomial fitting technique was employed to approximate the logarithmic temporal evolution of pixels, enabling the synthesis of data based on the resulting coefficients, as suggested by Shepard et al. (Shepard et al., 2001). The synthetic data, as shown in Fig. 4, reproduces the authentic thermal characteristics of the signal, effectively mitigating high-frequency noise components. Signal processing, e.g. the Fast Fourier Transform (FFT), performed on the synthetic data does not introduce additional noise, thus enhancing the efficiency of further data analysis. Another advantage is the reconstruction of the complete temporal evolution of a pixel using only the derived coefficients. This reduces storage demands and makes the overall computational process more efficient, therefore playing an important role for time critical on-the-fly sorting of plastics. In addition, the use of synthetic data allows us to mitigate some other artifacts, such as camera reflections, observed in a circular region directly beneath the camera. The uncooled camera heats up during use, reaching temperatures of about 40 °C. This heat (infrared radiation) is then reflected on the surface of a sample and, depending on the incident angle, sent back into the lens of the camera. These artifacts are prominent as an erroneous elevation roughly in the middle of the cooling curve, i.e. in the region where the samples are halfway along the camera view, as illustrated in Fig. 4.

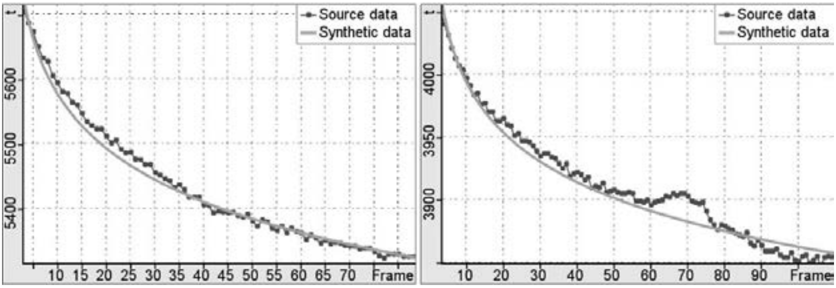

Fig. 4: Cooling curve source data and synthetic data; left: without artifacts, right: camera reflection artifact at frames ~60-75; a subset of the total of 136 frames

The FFT was applied to the cooling curves, as suggested by Maldague & Marinetti (Maldague & Marinetti, 1996) and widely adopted in related studies. The phase shift and amplitude information extracted via FFT helps to distinguish materials based on their thermal response (as shown in Fig. 5 and Fig. 6), avoiding the complexity of directly examining and comparing the cooling curves.

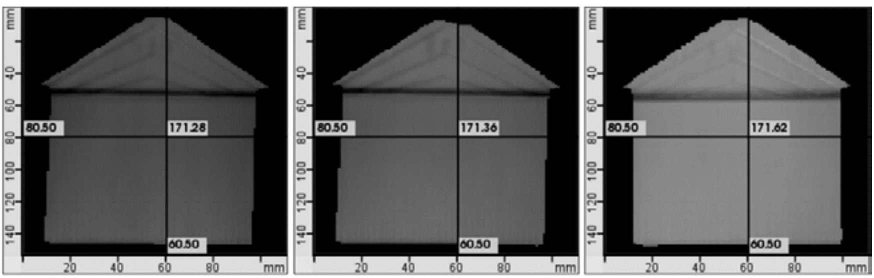

Fig. 5: FFT phase images (first frequency bin after DC) for PA66-GF, PA6-GF and PP-GF samples

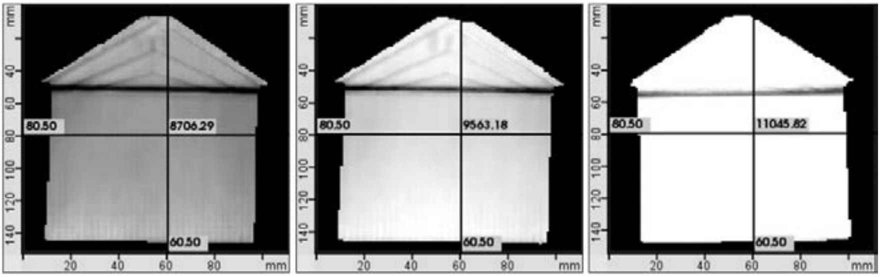

Fig. 6: FFT amplitude images (first frequency bin after DC) for PA66-GF, PA6-GF, and PP-GF samples

Different features and parameters were evaluated, considering their influence on the machine learning model's effectiveness. A comparison of FFT results obtained using source and synthetic data proves the effectiveness of the chosen approach. Through a series of extensive tests involving polynomials and derivatives of different orders, their outcomes were systematically compared, identifying the most effective parameters for further analysis. In addition to FFT-related features, it has proved useful to calculate the relative temperature drops by putting different target frames in relation to the initial frame, where an example for different materials is shown in Fig. 7. The following features were identified as the most significant and were selected as the input for the machine learning model:

- FFT amplitude (first 10 frequency bins after DC)
- FFT phase (first 10 frequency bins after DC)
- relative temperature drop for target frames 10, 20, 50, 80 and 90
- two polynomial coefficients (first-order polynomial in the logarithmic domain)

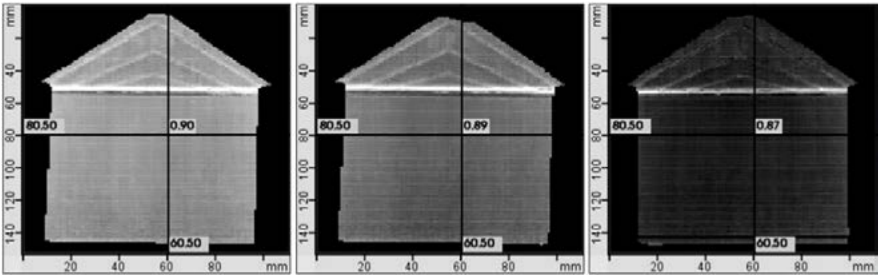

Fig. 7: Relative temperature drop for PA66-GF, PA6-GF and PP-GF samples, target frame 80

Data inspection

The analysis of the data initially begins with a univariate perspective. In this particular case, where the potential influences are largely suppressed, a univariate approach already can be effective in solving the classification problem. By looking at individual variables in isolation, this method enables a comprehensive understanding of the contribution of each factor and provides valuable initial insights. With these insights, a foundation is established for more complex analyses and a deeper understanding of the underlying patterns. Fig. 8 shows the value of one feature (first amplitude of the FFT) for each material. This approach would already allow a partial classification. However, in order to obtain a more accurate and stable prediction, all available features should be taken into account.

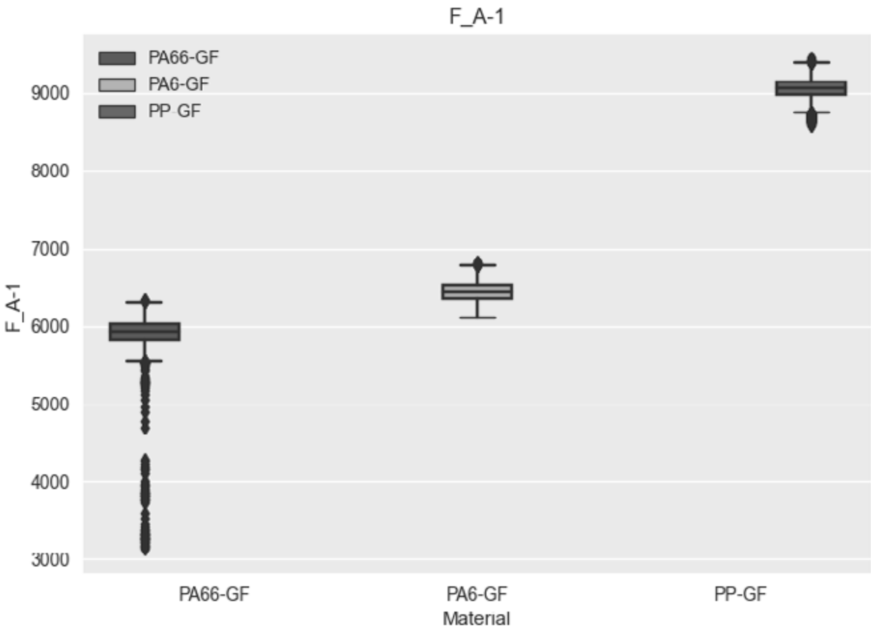

Fig. 8: First amplitude feature A-1 extracted from all samples

To inspect the multidimensional space of the dataset, different machine learning methods are applied using Python (version 3.8.10) and the Scikit-learn library (version 1.2.2) (Pedregosa et al., 2011). A multivariate technique that can be used is the Principal Component Analysis (PCA) (Jolliffe, 1986). PCA is generally used for dimensionality reduction. However, by analyzing the newly generated components, this algorithm can be applied to identify the most influential factors in the data set. This capability enables the identification of previously unseen or unknown influencing factors when designing the experiment. As the PCA is unsupervised, it is not trained to differentiate between classes. However, observing the differentiation of different classes in the newly generated principal components demonstrates the ability of this measurement setup to achieve material separation. Fig. 9 illustrates the first and second principal components, visually distinguishing the classes with different shapes. In the figure shown, only every 60th point is displayed for visibility reasons. Except for outliers in the top right, the difference between PP-GF and both PA-GF's is the highest influence in the dataset.

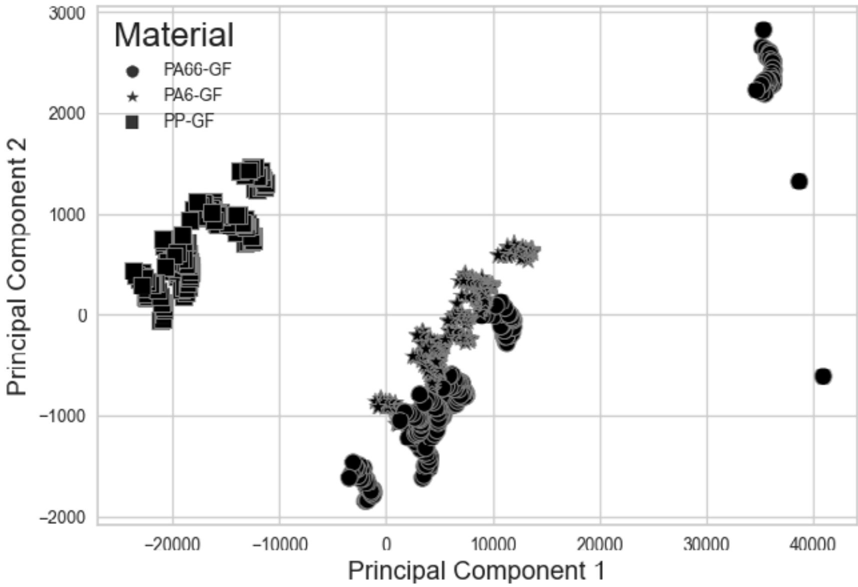

Fig. 9: Dataset plotted over two principal components (every 60th point for visibility)

4.2 Classification model

To create a machine learning model capable of distinguishing between three black plastic materials, the dataset is divided into training and validation sets. The validation set includes three complete samples that have been selected manually for each material. A pipeline is created containing a standard scaler followed by a linear discriminant analysis (LDA) (Fisher, 1936), which is a supervised method of multivariate statistics. During the training phase, the model is taught with the training dataset. Using the validation data, a transformation of the higher dimensional dataset is projected onto two new axes, called canonical variables (Fig. 10). In comparison to the unsupervised method (PCA) before, this projection with a supervised method improves the separation of the different materials. In this illustration, the classes are represented by different symbols. The distinction between PP-GF and the two PA materials is very clearly recognizable. Even PA6-GF and PA66-GF are mostly separable but have a slight overlap.

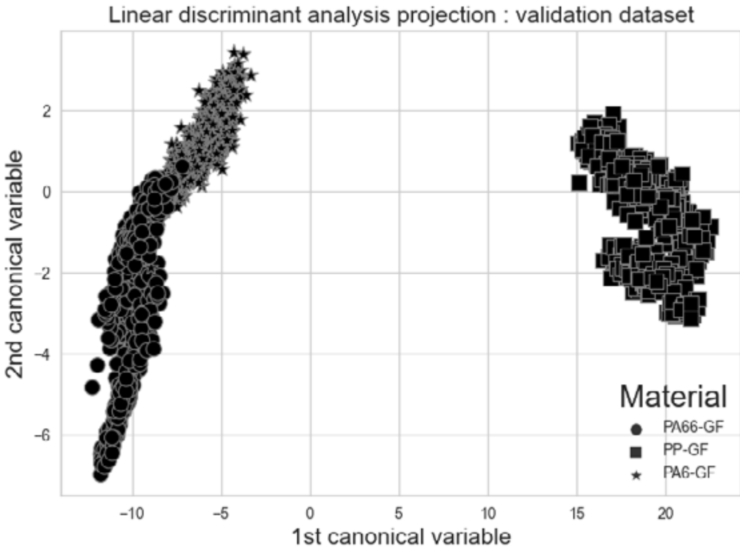

Fig. 10: Projection of the validation dataset in two new canonical variables

To measure the accuracy of the predicted results, a commonly used score is the f1-score. The f1-score combines precision and recall, its calculation is described in Fig. 11 (Fawcett, 2006).

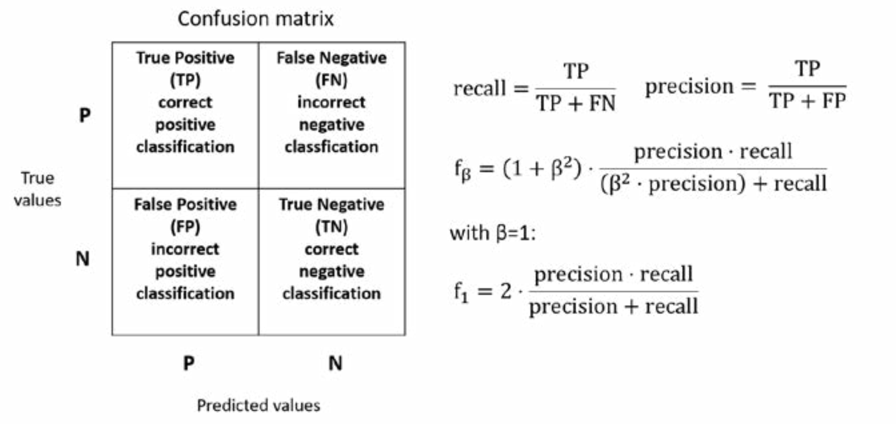

Fig. 11: Calculation of the f1-score

As shown in Fig. 12, an averaged f1-score of 0.985 could be achieved. Challenges in the prediction accuracy can be observed only between the materials PA6-GF and PA66-GF, which have very similar physical and chemical properties. However, the discrimination between PA6-GF/PA66-GF and PP-GF can be performed with perfect precision, achieving 100% accuracy.

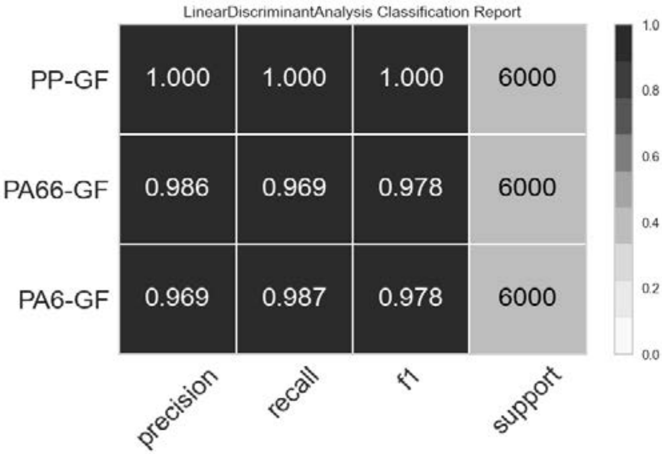

Fig. 12: Classification report of the validation dataset

Since pixel-wise sorting is infeasible, a strategic approach is to make a majority decision for each sample. Fig. 13 shows the confusion matrices in which the pixel-wise predictions (left) and the results obtained from majority decision per sample (right) are compared. The use of the majority decision method has led to an accurate classification of each sample.

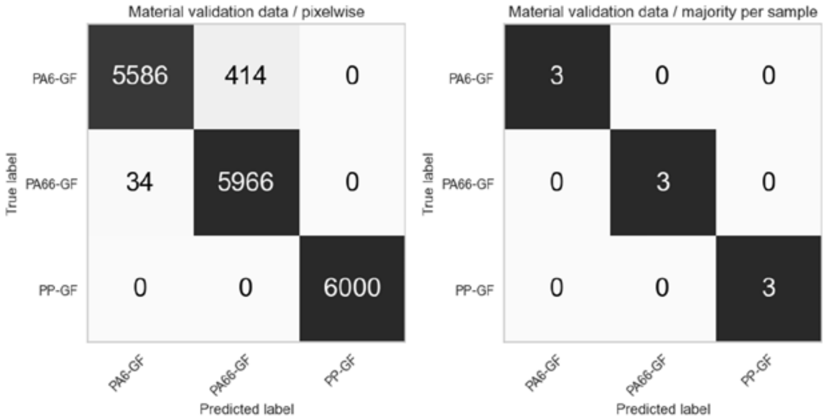

Fig. 13: Confusion matrices; left: pixel-wise, right: majority per sample

5 Conclusion and outlook

In this paper, an attempt has been made to classify black plastic materials (PA6-GF, PA66-GF, PP-GF) using active thermography. A setup has been developed that enables stable and defined measurements. All influencing factors were identified and classified, with the goal of reducing unknown and unwanted influences. Through iteratively improved pre-processing techniques, a machine learning model was created that demonstrated the capability to correctly classify all validation samples. In doing so, it has been shown that the current state of the art in sorting plastics can be improved through the application of this technology.

The next steps involve using this laboratory setup and the knowledge gained to add more and more of the real-world influencing factors, which were previously excluded (most importantly: different ambient temperatures, and different sample geometries). A calibration and temperature correction for the acquired signals can be trained and performed, increasing the stability of the data. In addition, the camera can be substituted to allow an increase of the belt speed through a higher frame rate. A camera with a higher resolution can also improve the quality and precision of the analysis, which is important for smaller sample sizes in the future. Another challenge is to reduce the self-reflection effects of the camera. This can be done, e.g. by placing the camera at an angle instead of vertically. In this case, the recorded images must be rectified using a corresponding geometric transformation. Also ongoing is the fusion of active thermography in the »Waste 4 Future« project into a demonstrator including other modalities, creating a multimodal sorter for plastic materials. As shown in this paper, the active thermography approach is capable of increasing the accuracy of classification on black plastics.

References

Aujeszky, T., Korres, G., & Eid, M. (2017). Thermography-based material classification using machine learning. In *2017 IEEE International Symposium on Haptic, Audio and Visual Environments and Games (HAVE)*.

Brandt, C., Kieninger, M., Negara, C., Gruna, R., Längle, T., Küter, A., & Nüßler, D. (2016). *Sorting of black plastics using statistical pattern recognition on terahertz frequency domain data*. https://publica.fraunhofer.de/handle/publica/391776

Chen, X., Kroell, N., Feil, A., & Pretz, T. (2020). Determination of the composition of multilayer plastic packaging with NIR spectroscopy. *Detritus*, *13*, 62–66. https://doi.org/10.31025/2611-4135/2020.14027

EC. (2020). *Circular Economy action plan.* Euopean Comission. https://environment.ec.europa.eu/strategy/circular-economy-action-plan_en

Fawcett, T. (2006). An introduction to ROC analysis. *Pattern Recognition Letters*, *27*(8), 861–874. https://doi.org/10.1016/j.patrec.2005.10.010.

Fisher, R. A. (1936). The use of multiple measurements in taxonomic problems. *Annals of Eugenics*, *7*(2), 179–188. https://doi.org/10.1111/j.1469-1809.1936.tb02137.x

Gundupalli, S. P., Hait, S., & Thakur, A. (2017). A review on automated sorting of source-separated municipal solid waste for recycling. *Waste Management*, *60*, 56–74. https://doi.org/10.1016/j.wasman.2016.09.015

Jehanno, C., Alty, J. W., Roosen, M., Meester, S. de, Dove, A. P., Chen, E. Y.-X., Leibfarth, F. A., & Sardon, H. (2022). Critical advances and future opportunities in upcycling commodity polymers. *Nature*, *603*(7903), 803–814. https://doi.org/10.1038/s41586-021-04350-0

Jolliffe, I. T. (1986). *Principal Component Analysis*. Springer Science. https://doi.org/10.1007/b98835

Jones Roger W., & McClelland John F. (1989). Transient infrared emission spectroscopy. *Analytical Chemistry*, *61*(7), 650–656. https://doi.org/10.1021/ac00182a003

Maldague, X., & Marinetti, S. (1996). Pulse phase infrared thermography. *Journal of Applied Physics*(79), 2694–2698. https://doi.org/10.1063/1.362662

Masoumi, H., Safavi, S. M., & Khani, Z. (2012). Identification and classification of plastic resins using near infrared reflectance. *International Journal of Mechanical Sciences*, *6*, 213–220.

matweb. https://www.matweb.com/index.aspx

Menczel, J. D., & Prime, R. B. (2009). *Thermal Analysis of Polymers: Fundamentals and Applications*. John Wiley & Sons, Inc. https://doi.org/10.1002/9780470423837

Olscher, C., Jandric, A., Zafiu, C., & Part, F. (2022). Evaluation of Marker Materials and Spectroscopic Methods for Tracer-Based Sorting of Plastic Wastes. *Polymers*, *14*, 3074. https://doi.org/10.3390/polym14153074

Pedregosa, F., Varoquaux, G., Gramfort, A., Michel, V., Thirion, B., Grisel, O., Blondel, M., Prettenhofer, P., Weiss, R., Dubourg, V., Vanderplas, J., Passos, A., Cournapeau, D., Brucher, M., Perrot, M., & Duchesnay, E. (2011). Scikit-learn: Machine Learning in Python. *Journal of Machine Learning Research*, *12*, 2825–2830.

Polysecure GmbH. *Polysecure*. https://www.polysecure.eu/en/sort-reliably/tracer-based-sorting

Rozenstein, O., Puckrin, E., & Adamowski, J. (2017). Development of a new approach based on midwave infrared spectroscopy for post-consumer black plastic waste sorting in the recycling industry. *Waste Management*, *68*, 38–44. https://doi.org/10.1016/j.wasman.2017.07.023

Schmidt, J., Grau, L., Auer, M., Maletz, R., & Woidasky, J. (2022). Multilayer Packaging in a Circular Economy. *Polymers*, *14*(9). https://doi.org/10.3390/polym14091825

Sensors Unlimited. https://www.sensorsinc.com/applications/machine-vision/plastic-sorting

Shepard, S. M., Ahmed, T., Rubadeux, B. A., Wang, D., & Lhota, J. R. (2001). Synthetic processing of pulsed thermographic data for inspection of turbine components. *Insight: Non-Destructive Testing and Condition Monitoring*, *43*, 587–589.

Stegmann, P., Daioglou, V., Londo, M., van Vuuren, D. P., & Junginger, M. (2022). Plastic futures and their CO2 emissions. *Nature*, *612*(7939), 272–276. https://doi.org/10.1038/s41586-022-05422-5

W4F. *Waste 4 Future.* Fraunhofer-Gesellschaft. https://www.waste4future.fraunhofer.de/en.html